

SBC2007-176295

**NONLINEAR FINITE ELEMENT MODELING OF
MONKEY POSTERIOR SCLERA UNDER INTRAOCULAR PRESSURE**

**Michaël Girard (1), Crawford J. Downs (2), Claude F. Burgoyne (2),
Michael Bottlang (3), and Jun-Kyo F. Suh (1)**

(1) Department of Biomedical Engineering
Tulane University
New Orleans, Louisiana

(2) Devers Eye Institute
Legacy Health System
Portland, Oregon

(3) Legacy Research & Technology Center
Biomechanics Laboratory
Portland, Oregon

INTRODUCTION

We hypothesize that the mechanical properties of posterior sclera play a central role in the development of glaucomatous vision loss.

In order to evaluate the effect of intraocular pressure (IOP) on the connective tissues of the posterior pole and optic nerve head (ONH), it is essential to fully characterize the mechanical behavior of each tissue within and around the ONH.

The sclera is the outer shell and principal load-bearing tissue of the eye. Consisting primarily of collagen fibers and being essentially avascular, it provides constant protection for the underlying intraocular tissues.

In our previous study [1], experimental and mathematical models were developed to determine the mechanical properties of the sclera, using a uniaxial tensile testing protocol. However, sclera is a highly complex structure with varying collagen fiber orientation and one may have to look deeper in its microstructure to gain a better understanding of its behavior under mechanical stress such as IOP. Uniaxial testing becomes then insufficient to predict the mechanical behavior of the tissue in vivo. A more physiological protocol is necessary to fully describe the 3-D behavior of the sclera under IOP.

This current report is presenting a method to experimentally characterize the 3-D deformation pattern of monkey posterior sclera and to determine its nonlinear and anisotropic material properties due to acute elevation of IOP from 5 to 45 mm Hg.

MATERIAL AND METHODS

Experimental Set Up and Testing Protocol

The left eye of a rhesus monkey was stored in a phosphate buffered solution (PBS) at 22°C for 3 hours. At the time of the experiment, the anterior chamber and vitreous of the eye were removed, and the posterior scleral shell was mounted and clamped at

the equator on a custom-built pressurization apparatus which allowed the specimen to be pressurized with a column of PBS with a resolution of 0.1 mm Hg (Figure 1). Before the experiment, the pressurized scleral sample was blotted, covered with a white titanium powder to enhance surface roughness, and immersed in PBS. IOP was slowly increased by incremental steps of 0.1 mm Hg, from 5 to 45 mm Hg, and the 3-D displacement field of the posterior sclera was measured at equilibrium using an electronic speckle pattern interferometry (ESPI) sensor (Ettemeyer AG, Q100) suspended over the scleral sample.

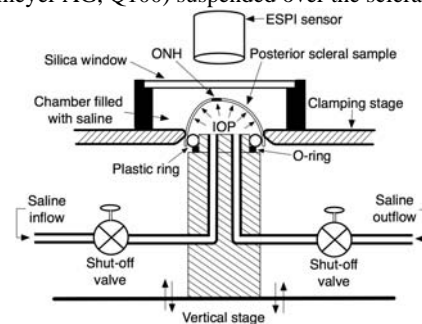


Figure 1. Schematic of the pressurization apparatus.

The ESPI sensor (resolution: ~ 0.1 μm; field of view: 35 mm × 25 mm) captured laser speckle images from 4 independent illumination directions for each pressure incremental step [2]. Speckle image subtraction and fringes analysis algorithms (Ettemeyer AG, ISTR A Q100 V2.7) were employed to extract the 3 displacement components (i.e. x, y and z) of the displacement field. Each component was reported in a 256 × 256 matrix that covered a 20 mm × 20 mm region. Hence, 3-D displacements were obtained for the pressure changes

from 5 mm Hg to 10 mm Hg, from 10 mm Hg to 30 mm Hg, and from 30 mm Hg to 45 mm Hg. The outer surface geometry of the scleral shell was digitized using with a 3-D digitizer arm (MicroScribe, G2X), and the scleral thickness was measured at predetermined locations throughout the entire shell with a 20 MHz ultrasound transducer (Sonomed, Inc., PacScan 300P).

Anisotropic and nonlinear modeling

Outer surface geometry and thicknesses data were combined in order to reconstruct the anatomical posterior geometry of the shell, and to create a 8 noded-finite element (FE) mesh which was further divided into 9 regions (Figure 2).

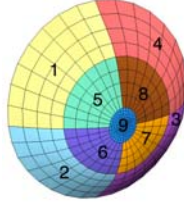


Figure 2. FE mesh of the posterior scleral shell. Regions (1-4) are the peripheral sclera, Regions (5-8) are the peripapillary sclera, and Region 9 is the ONH.

Scleral collagen fiber alignment was assumed to be distributed within a plane tangent to the shell surface at each material point, with a statistical probability distribution P , known as semi-circular Von Mises distribution (Figure 2):

$$P(\theta) = \frac{1}{\pi I_0(k)} \exp(k \cos(2(\theta - \theta_p))) \quad (1)$$

where I_0 is the modified Bessel function of the first kind (order 0), θ_p is the principal orientation of the collagen fibers and k is defined as the fiber concentration factor.

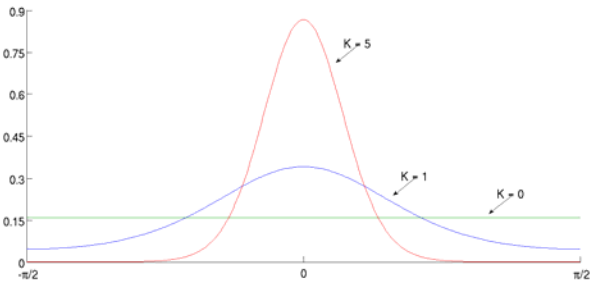


Figure 3. Variation of the probability function $P(\theta)$. As k increases the fibers align in a unique direction, here $\theta_p=0$.

The probability distribution P was incorporated into the scleral strain energy function W_{sclera} defined as:

$$W_{sclera} = W_{matrix} + \int_{\theta_p - \frac{\pi}{2}}^{\theta_p + \frac{\pi}{2}} P(\theta) W_{fiber}(\theta) d\theta \quad (2)$$

where W_{matrix} is an isotropic contribution from the proteoglycan-based ground matrix, and W_{fiber} is an anisotropic contribution from the collagen fiber family in the direction of θ [3]. The model was implemented within the software NIKE3D, which is a nonlinear and implicit FE code for solid mechanics.

Three parameters were uniformly attributed to the entire scleral FE mesh ($c1$: Mooney-Rivlin matrix coefficient, $c3$: exponential fiber stress coefficient, and $c4$: fiber uncrimping coefficient). Two fiber concentration factors, $k1$ and $k2$, were attributed to the peripheral sclera (Regions 1-4) and to the peripapillary sclera (Region 5-8),

respectively. A total of eight principal fiber orientation parameters, θ_{p1} to θ_{p8} , were attributed to each scleral region, respectively. The ONH was assumed to be an incompressible, isotropic material with an elastic modulus fixed to 0.1 MPa.

Using our NIKE3D model, surface node displacements were curve-fitted to the experimental data simultaneously at 10, 30 and 45 mm Hg using a genetic optimization algorithm [5], which estimated a unique set of 13 material parameters as defined previously.

RESULTS

Experimental displacement field was nonlinear and well matched by the proposed model (Figure 3-A, x-displacement shown as example). The matrix modulus, $c1$, was 0.35 MPa and the initial fiber modulus was 3.9 MPa ($c3 \times c4$), which is consistent with fiber moduli reported in previous studies. The model predicted predominant collagen fiber orientation to be circumferential in the peripapillary sclera region (Figure 3-B), which matches reported histologic results [4].

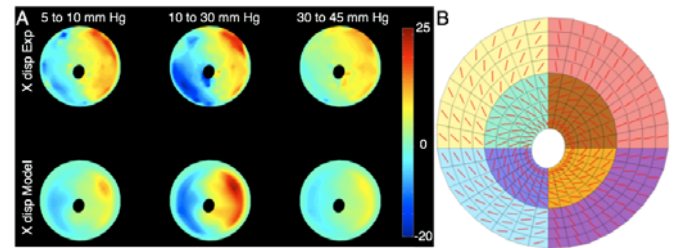


Figure 4. (A) Experimental x displacement using ESPI and model prediction (in microns). (B) Predicted predominant collagen fiber orientation.

DISCUSSION

Posterior scleral deformation following acute IOP elevations appears to be non-linear and governed by the underlying scleral collagen microstructure as predicted by FE modeling. This preliminary study is the first 3-D modeling of scleral mechanics. The method will now be used to characterize scleral mechanics in normal (young and old), early glaucomatous and moderately glaucomatous monkey eyes.

ACKNOWLEDGMENT

The authors would like to thank Dr. Michael Puso, from the Lawrence Livermore National Laboratory, for allowing them to use and implement their model within the nonlinear FE code NIKE3D.

REFERENCES

- Downs, J. C., Suh, J-K. F., Thomas, K. A., Bellezza A. J., Burgoyne, C. F., and Hart, R. T., 2003, "Viscoelastic characterization of peripapillary sclera: material properties by quadrant in rabbit and monkey eyes," J Biomech Eng, 125, pp. 124-31.
- Erne, O. K., Reid, J. B., Ehmke, L. W., Sommers, M. B., Madey, S. M., and Bottlang, M., 2005, "Depth-dependent strain of patellofemoral articular cartilage in unconfined compression," J Biomechanics, 38, pp. 667-672.
- Weiss, J. A., Maker, B. N., and Govindjee, S., 1996, "Finite element implementation of incompressible, transversely isotropic hyperelasticity," Comput Methods Appl Engr, 135, pp. 107-128.
- Kokott W., 1934, "Das spatlinienbild der sklera, ein beitrag zum funktionellen bau der sklera," Klin Mbl Augen, 92, pp. 177-185.
- Price, K.V., Storn, R. M., Lampinen J. A., 2005, *Differential evolution*, Springer-Verlag, Berlin.